UNIVERSITÄT AUGSBURG
Universitätsbibliothek

OPEN ACCESS
OPUS AUGSBURG

Localization of acoustic emission sources in fiber composites using artificial neural networks

Sinan Kalafat, Markus G. R. Sause

Angaben zur Veröffentlichung / Publication details:

Kalafat, Sinan, and Markus G. R. Sause. 2014. "Localization of acoustic emission sources in fiber composites using artificial neural networks." In *31st Conference of the European Working Group on Acoustic Emission (EWGAE), 3 - 5 September 2014, Dresden, Germany*. Berlin: DGZfP.

Nutzungsbedingungen / Terms of use:

CC BY-ND 4.0

Dieses Dokument wird unter folgenden Bedingungen zur Verfügung gestellt: / This document is made available under these conditions:
CC-BY-ND 4.0: Creative Commons: Namensnennung - Keine Bearbeitung
Weitere Informationen finden Sie unter: / For more information see:
https://creativecommons.org/licenses/by-nd/4.0/deed.de

More Info at Open Access Database www.ndt.net/?id=17530

Localization of Acoustic Emission Sources in Fiber Composites Using Artificial Neural Networks

Sinan KALAFAT, Markus G. R. SAUSE
University of Augsburg, Institute for Physics, Augsburg, Germany

Abstract. The localization of acoustic emission (AE) source positions is an important concept used for failure detection and material characterization. However classical localization techniques often provide misleading localization results in anisotropic fiber composites, media with internal discontinuities or due to incident reflections at the sensor position. As an alternative strategy to fixed localization schemes, we recently proposed an artificial neural network (ANN) based approach to improve the accuracy of AE source localization in fiber reinforced composite structures. This method offers the advantage of an adaptive modelling based on experimental data. Three plate like test specimens made of the thermoplastic carbon fiber reinforced composite T700/PPS with different dimensions were used for load bearing tests in combination with AE acquisition. We varied the thickness of the three specimens systematically to gain a ratio in the characteristic lengths from one to two to three. Therefore Lamb wave propagation in the thickest plate is expected to be systematically different from the wave propagation in the thinnest plate and is subject to mode specific propagation velocities and dispersion. In addition, the bolts used for load introduction disturb the signal propagation between AE source and AE sensors. This often causes erroneous AE source localizations using classical methods. In the present study, the localization quality in all structures investigated is presented in comparison between state-of-the-art methods and the neural network based method. We present results to quantify the absolute deviation of the two methods for known acoustic emission source positions using different wave excitation methods to simulate AE signals of different failure mechanisms. The two excitation methods vary distinctly in their AE signal characteristics and cause generation of different ratios of Lamb wave modes. The influence of these different Lamb wave modes on the localization accuracy will be discussed. Further, the application of both localization methods is presented in application on measurement data from load bearing tests of each geometry type. It could be demonstrated that the neural networks based approach provides better results compared to the classical methods.

1. Introduction

The application of fiber reinforced polymers (FRP) as lightweight construction material offers the possibility of free form design as well as an application specific optimum of strength and stiffness in combination with a low density. Moreover, composites offer many other advantages such as corrosion resistance, high specific energy consumption as well as

License: http://creativecommons.org/licenses/by-nd/3.0/

an adjustable electrical conductivity over wide ranges [1]. Therefore, these high-performance materials show an increasingly broad range of use. However, designing materials with such anisotropic stiffness also leads to an anisotropic sound velocity.

In general, FRP are used as thin-walled structures, such as plates, cylinders or rods. The way of acoustic signal propagation in such structures is a type of guided wave, for plates referred to as Lamb waves. The propagation velocities of the respective Lamb wave modes show high dependence on the direction of propagation. In addition, there is a variance of the acoustic emission (AE) signals in composite materials which depends on the acoustic emission source characteristics, i.e. due to matrix cracking or fiber breakage [2]. All of these effects can cause systematic localization errors, especially for localization methods assuming isotropic sound velocities.

Therefore, new methods providing more accurate source localization procedures are highly appreciated for testing of composite materials. This is often achieved by improvement of classical methods or by aid of simulation approaches [3] [4] [5]. However, for a broad application, it is advantageous to develop a source localization method which is universally applicable and provides accurate results in arbitrary geometries. In the following, we demonstrate how neural networks can be used for AE source localization. The proposed method is demonstrated in application to three fiber reinforced plates of different size as typically used for testing of bearing strengths. This setup is particularly challenging for any source localization algorithm, since the bolts used for load introduction allow only indirect signal propagation paths between some of the source positions and the sensors.

2. Methodology

In the following we first introduce the classical source localization method and present our new approach for source localization using neural networks. Subsequently, details of the experimental setup used for the load bearing tests are presented.

2.1 Classical source localization method

The Δt method uses the arrival time difference of waves detected at two sensors as input quantity. Using the formula:

$$|\vec{r_i} - \vec{r_0}| = c\,(t_i - t_0) \qquad (1)$$

the source location $\vec{r_0}$ of the acoustic emission can be calculated. In equation (1) c is the propagation speed and the respective sensor locations $\vec{r_i}$ use the arrival times t_i at the respective sensor location. This formula is valid for two-dimensional systems. Since the components used here are plate structures, equation (1) can be applied. It can be seen from the structure of equation (1) that the output is a hyperbola of spatial vector length at equal arrival time differences. For this reason, three sensors are required to yield unique intersection point of the hyperbolas to perform a 2D source localization. Also, equation (1) uses a constant sound velocity c. It is possible to modify this equation, if a known bi-directional velocity characteristic is present in the investigated object. This advanced method will be applied in the following results. As a solution procedure for the respective equation system Nelder-Mead algorithms [6] are used. All results obtained by this Δt method serve as a benchmark and will be referred to as classical approach in the following [7].

2.2 Neural network source localization method

The use of artificial neural networks (ANN) is usually divided into two phases. The first phase is referred to as model building or training phase, where the ANN is conditioned to a representative dataset. For the case of AE source localization, a complete set of input data consists of the arrival time differences between the sensors and their respective source positions. It must be ensured that the database used to build the model is representative and is fully descriptive of the system. Complex geometric shapes, acoustic invariances as well as mechanically stressed areas therefore require a higher density of training data points [8] [9]. Based on this training data, a function is approximated that includes all characteristics of the system. In the second phase, this function can be used to approximate any unknown AE source positions based on the measured arrival time differences. The advantage of this method is that it can approximate the properties of arbitrary systems, even if no analytic formula is able to perform source localization in such a structure. A similar approach has been followed by the group around Blahacek in [10] and Scholey [11] [12].

The individual components of a neural network are called artificial neurons which are linked via coupling weights. The weight of the couplings is changed by approximating the information provided by the training data set. As a learning rule suitable for the AE source localization procedure, supervised learning algorithms are used [13] [14] as they typically provide consistent and convergent networks. For such supervised learning, the classical backpropagation neural network is used as training algorithm as well as derivatives such as resilient backpropagation or superSAB [13]. In this case, the ANN is divided into individual layers with an arbitrary number of neurons. Each neuron has a connection to all the neurons of the subsequent layer which is known as a feed-forward network. This leads to a certain network output which is compared with the known target output (the known AE source location). The resulting deviation between the computed positions and the known positions is fed back to the network which gradually changes the weights to minimize the deviation. If the network output at a specific input dataset is sufficiently close to the target output the network is considered as trained and can therefore be used to approximate unknown AE source positions. In the context of AE source localization, two layer networks are used which can have 2-50 neurons per layer. The individual neurons use a sigmoidal activation function.

3. Experimental Setup

Three types of load bearing test specimens with different dimensions are investigated. The smallest specimen has a quasi-isotropic stacking sequence with the dimensions 108 mm x 54 mm x 22 mm (height x width x thickness). The specimen has two holes with a diameter of 9 mm each about 31 mm from the edge. For load introduction, bolts were placed in these holes as depicted in figure 1. For the remaining two plates all geometrical dimensions were scaled by a factor of two and three, respectively.

As acoustic emission sensors four WD type sensors were used. These are coupled to the specimen by a medium viscosity silicone grease using clamps for the sensor position at the edges of the plates. The sampling rate is 10 MS/s with a preamplification factor of 40 dB_{AE}. The threshold was set to 35 dB_{AE} and the waves were filtered using a band-pass ranging from 20 kHz to 1 MHz.

As training data matrix for the neural network source localization, a rectangular grid of 1 cm ± 0.7 mm is used for each of the specimen types. Therefore specimens of different sizes have a different number of training signals as data base. The training data was low-pass filtered using a 3rd order Butterworth filter with 120 kHz cut-off frequency.

In previous work [9] it was shown that the localization quality of neural networks in CFRP plates with increasing anisotropy is superior to the localization quality of the classical method. In extreme cases, such as a unidirectional plates, the localization results were improved by a factor of 13. To achieve such a localization accuracy every structure had its own set of training data points and a set of test points which were created in the same setup. However, to investigate the scalability and portability of trained networks, only one database will be used for the results shown herein. This database was generated using the medium size plate. Since the three different plates vary in all dimensions by a factor of 2 and 3 relative to the smallest plate, the Δt values of the training dataset are multiplied by the respective factors. When compared to the training datasets recorded for the smallest and largest plate no substantial differences to the scaled training dataset were observed.

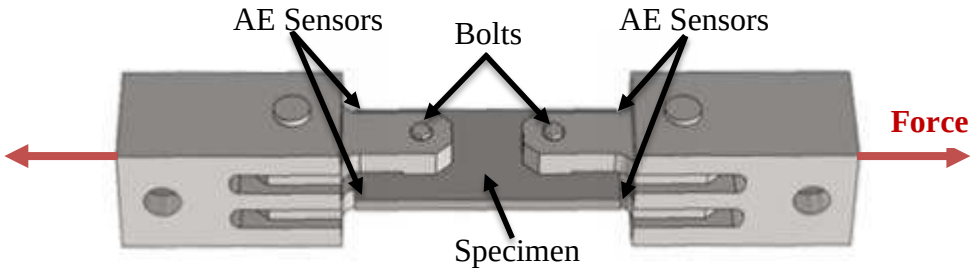

Fig. 1. Exemplary illustration of the experimental setup

Test signals are generated with a classical Hsu-Nielsen source [14] using a lead diameter of 0.5 mm and hardness 2H. The length of the pencil lead is 3 mm ± 0.5 mm. This test signal source preferably produces signals with low frequency content. In order to generate test signals representative for the full range of possible experimental signals during material failure, it is necessary to also generate signals with higher frequencies [2]. These signals are generated by a short electrical pulse applied to a piezoelectric actuator. The pulses are created using an arbitrary waveform generator using an edge width of 20 ns and a pulse width of 10 µs at a maximum of 10 V. The piezoelectric actuator generates a force pulse which then stimulates an acoustic emission signal with broad band-width.

The bandwidth of the pencil lead breakage signals was found to range from 200 kHz to 400 kHz, while the bandwidth of the pulser reaches from 350 kHz to 800 kHz. It can thereby be ensured that for the training of the neural network, arrival times of all relevant modes are accounted for. As input or general location basis, the time differences are used which are extracted by threshold or the AIC criterion from the waves [15] [16]. The choice between the two is depending on the method that provides the least strong outliers.

Experimentally it has been found that for the evaluation of the localization accuracy only the Δt arrivals are suitable which can be clearly assigned to one event. This is done by filtering the measured Δt values to assure all mutual Δt pairs are below a certain realistic Δt value. Measurement data from continuous emissions are also omitted from the analysis.

4. Comparison of source localization results

In the following we compare the results as obtained by the classical Δt method to the application of the neural network based method.

4.1 Quantification of source localization accuracy

To quantify the localization accuracy, it is important to know the real position of the sources. Since this is limited in the case of a measurement loading the specimen to failure, the localization accuracy of the two methods is compared in one structure using artificial

test sources as used for the training datasets. A total of 210 data points were generated each on a square pattern with 1 cm edge distance. From this data the Δt values were extracted whereas those records with unrealistic Δt values are sorted out. For the classical method, the test sources were localized with an anisotropic velocity distribution with 4190 m/s in the horizontal direction and 5320 m/s in the vertical direction. The result of the measured localization accuracy is shown in figure 2. For each test source position, the corresponding deviation between the test source position and the localization result (localization accuracy) is indicated as false-color range. This is shown for the classical method and the neural method using a Hsu-Nielsen source in figure 2. The color coding in figure 2 shows a deviation from 0 cm (blue areas) to up to 3 cm (red areas). It can be seen, that the classical method shows significantly higher deviations over the entire plate. The resulting average total localization error on the plate with the classic method based on 161 localized test source points is 1.41 cm ± 0.54 cm. In comparison, the localization result of the neural method on the left uses 51 training data points and 110 test data. The average localization error of the neural network method is 0.47 cm ± 0.37 cm. Thus the neural method outperforms the classical method by a factor of three.

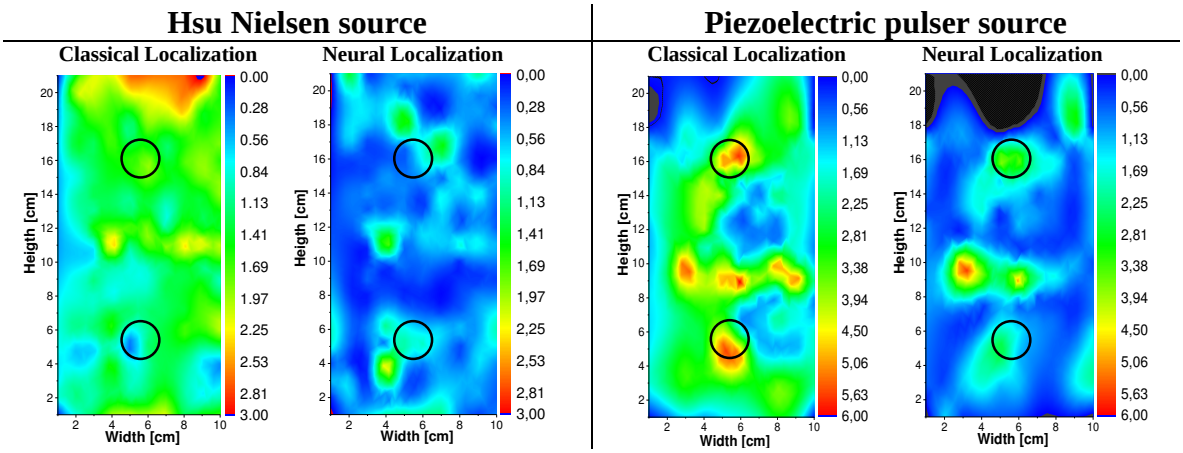

Fig. 2. Color code representation of localization error in cm showing acoustic emission events on a plate with two holes and the dimensions 216 mm x 108 mm x 44 mm for pencil lead breaks as test source (left) and piezoelectric pulser as test source (right).

Since acoustic emission events of higher frequency are also likely to occur during loading of fiber reinforced materials, the localization quality is also examined for signals with higher frequencies using the piezoelectric pulser as test source as seen in figure 2. The result is shown on the right side of figure 3. The localization error using the classical method is 2.31 cm ± 0.54 cm whereas the same set of input data using the neural network method reduces the localization error to 1.09 cm ± 0.37 cm. Since the excitation by a piezoelectric pulser is less intense than by the pencil lead break, only 125 data points could be used instead of 161. However, the average localization error is reduced in this case by a factor of two.

Since the neural network model is a fit of the symbolic link within a dataset, it is possible to determine the localization accuracy directly from the fit quality of the training procedure, assuming the data base is representative of the entire system. Thus by using all data points, the localization error can be further reduced to 0.3 cm by the pencil lead break source and to 0.7 cm by the piezoelectric pulser.

4.2 Results from tensile testing

Figure 3 shows the localization results using the classical and the neuronal method based on identical input data (i.e. identical Δt values). The left image shows the density of acoustic

emission source events using the classical method and on the right is the respective result of the artificial neural networks based method. Based on the test principle and on the visual observations during and after the test, the maximum damage occurs directly behind the loaded bolt. Therefore it is expected that the acoustic emission sources occur predominantly above the upper bolt and below the lower bolt.

It can be seen that the source positions obtained by the classical source localization method are scattered over the entire plate. For the small specimen 472 valid Δt sets were used. From these 472 data points, 188 data points were localized outside the plate by the classical source localization procedure. The algorithm used in the present investigation projects the data localized outside the defined range of interest to the edges of the plate. This causes the artefacts at the edges visible in figure 3. At the lower hole the maximum number of sources occurs. In contrast to the classical method, the right image shows the localization of the same data using the neural network based method. Here the distribution of source locations is significantly smaller. Also, an accumulation of acoustic emission sources above the top bolt is visible. At the lower bolt a much broader pattern of localized sources is evident. All 472 input sets were localized on the plate by the neural network based method, which means that there are no outliers present. In particular, all signals localized outside the plate by the classical method fall into the range now localized below the bolt.

In figure 4, the localization of the Δt values is shown on a plate for dimensions twice that of figure 3. However, only 105 valid input sets were recorded despite of the eight times higher specimen volume. This is caused by the increasing amount of continuous acoustic emission signals during loading. This substantially reduces the amount of signal sets with clearly detectable signal onsets. For the classical source localization method it is observed that almost all AE events were located at the bolt positions. In the neuronal network based source localization, however, the dense spots of the acoustic emission source positions are close to the expected damage position above the upper bolt and below the lower bolt.

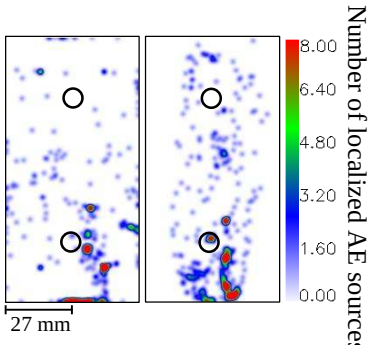

Fig. 3. Localization of 472 acoustic emission events on a plate with two holes and the dimensions 108 mm x 54 mm x 22 mm. left: Classical source localization procedure right: Neuronal source localization procedure

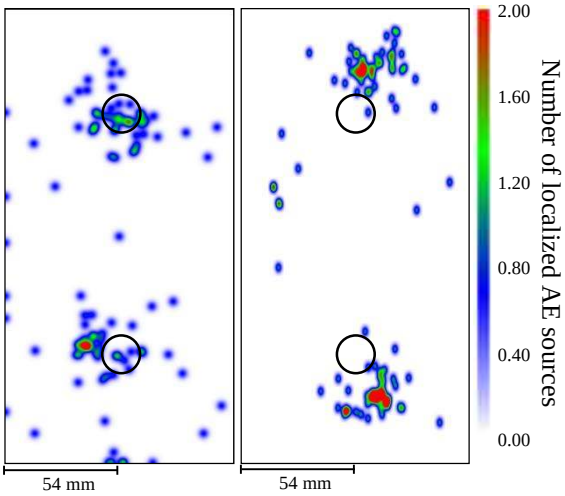

Fig. 4. Localization of 105 acoustic emission events on a plate with two holes and the dimensions 216 mm x 108 mm x 44 mm. left: Classical source localization procedure right: Neuronal source localization procedure

In the largest plate (Fig. 5) all dimensions are three times larger than in the smallest plate. Again, a significant reduction of valid Δt sets to 69 is found. This again attributed to the same effect as for the medium size plate. For the classical source localization method,

39 points are placed outside the plate, whereas the neuronal source localization procedure places only one source event outside the plate. The positions of localized sources are spread out more than for the other plates, but the localized positions resemble spots of visually observed damaged as well.

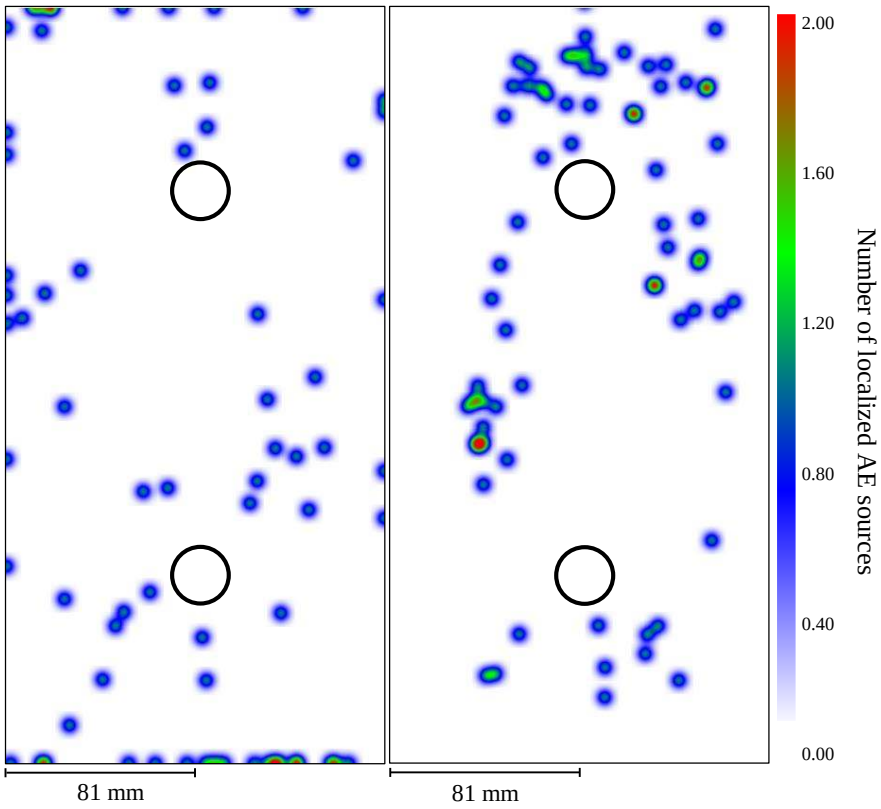

Fig. 5. Localization of 69 acoustic emission events on a plate with two holes and the dimensions 324 mm x 162 mm x 66 mm. left: Classical source localization procedure right: Neuronal source localization procedure

5. Discussion

Three planar samples of different sizes used for load bearing tests were examined using acoustic emission analysis. These plates were loaded until bearing failure and the acoustic emission events occurring during the load were localized using two different methods. A high acoustic emission density is expected directly along the load axis behind the bolts due to the notch effect. The classical Δt localization method showed a very wide spread of localized sources. In general, the acoustic emission events scatter strongly in all specimens and particularly in the small plate size 188 of 472 measured points are localized outside the plate. Particularly difficult is the localization directly below the bolt, since there is no direct propagation path between all four sensors. Therefore, the localization results in this area exhibit high errors using the classical source localization method. This problem is particularly well seen in the medium size specimen. Here most of the points are localized directly at the bolt positions, while the neural network based results are very close to the visually observed damage positions. Therefore it can readily be concluded, that the neural localization results are more meaningful. This impression is also confirmed in the investigations of the largest plate as well as the previous investigations on the localization accuracy with the artificial emission sources. It has also been proven that the localization accuracy of the neural network based source localization exceeds the classical Δt localization method up to a factor of three, where it is also possible to estimate the expected

average error on the basis of the neural network fit quality, which was evaluated to be between 0.3 cm and 0.7 cm for the present case.

It was demonstrated, that interferences of the wave field, such as reflections or geometric shapes can be accounted for using neural network based source localization approaches.

Acknowledgment

We thank the German Federal Ministry of Education and Research for the funding provided within the project MAI zfp within the leading edge cluster MAI Carbon.

References

[1] Mechanics of Composite Materials, R. M. Jones, 1998.
[2] Quantification of failure mechanisms in mode-I loading of fiber reinforced plastics utilizing acoustic emission analysis. M. G. R. Sause, T. Müller, A. Horoschenkoff, S. Horn Composite Science and Technology 72, 2012
[3] Acoustic Emission Source Location in Composite Aircraft Structures using Modal Analysis, D. Aljets, University of Glamorgan, 2011.
[4] Acoustic Emission Source Location in Plate-Like Structures using a closely arranged Triangular Sensor Array, D. Aljets, A. Chong, S. Wilcox, EWGAE, 2010
[5] Quantification of the Uncertainty of Pattern Recognition Approaches Applied to Acoustic Emission Signals. M. G. R. Sause, S. Horn, Journal of Nondestructive Evaluation 32 pp. 242-255, 2013
[6] A Simplex Method for Function Minimization, J. A. Nelder, R. Mead, Computer Journal, 1965
[7] Acoustic Emission Testing Basics for Research – Applications in Civil Engineering, C.U. Grosse, M. Ohtsu, Springer, 2008
[8] Lokalisierung von Schallemissionsquellen mit künstlichen neuronalen Netzwerken in Faserverbundwerkstoffen, S. Kalafat, Universität Augsburg, 2013
[9] Lokalisierung von Schallemissionsquellen in Faserverbundwerkstoffen mit künstlichen neuronalen Netzwerken, S. Kalafat, M. G. R. Sause, DGZfP-BB 142, 2013
[10] Neural network AE source location apart from structure size and material, M. Chlada, Z. Prevorovsky, M. Blahacek, J. Acoustic Emission, 28, 2010
[11] Two-dimensional source location techniques for large composite plates, J. J. Scholey, P. D. Wilcox, M. R. Wisnom, M. I. Friswell, Sep 2008 28th European Conference on Acoustic Emission Testing.
[12] A generic technique for acoustic emission source localization, J. J. Scholey, P. D. Wilcox, M. R. Wisnom, M. I. Friswell, M. Pavier, M. R. Aliha, J. Acoustic Emission, 27, 2009
[13] Neural Networks for Pattern Recognition, C. M. Bishop, Claredon Press - Oxford, 1995
[14] Investigation of pencil lead breaks as acoustic emission sources, M. G. R. Sause, Journal of Acoustic Emission 29, 184 – 196, 2011
[15] Markovian representation of stochastic processes and its application to the analysis of autoregressive moving average processes, H. Akaike, Annals of the Institute of Statistical Mathematics 26, p.363-387, 1974.
[16] Strategies for reliable automatic onset time picking of acoustic emissions and of ultrasound signals in concrete, J. H. Kurz, C. U. Grosse, H. W. Reinhard, Ultrasonics 43, p.538-546, 2004